

## The Oxidation of Rhodium Field-Emitter Surfaces during the CO Oxidation Reaction

G. L. KELLOGG

*Sandia National Laboratories, Albuquerque, New Mexico 87185*

Received August 22, 1984; revised November 20, 1984

The oxidation of Rh field-emitter surfaces during the CO oxidation reaction has been investigated by imaging atom-probe mass spectroscopy. Rhodium samples were heated to 500 K in various mixtures of O<sub>2</sub> and CO at total pressures between 1 and 2 Torr (1 Torr = 133.3 N m<sup>-2</sup>) and were subsequently transferred under ultrahigh vacuum to the atom probe for analysis. Surface oxides were detected when the O<sub>2</sub>/CO ratio was 40/1 or greater, but not when the ratio was 30/1 or less. The 40/1 ratio correlates with the ratio where deactivation of the reaction has been observed, and the results provide direct evidence that oxide formation is the surface process responsible for deactivation. Quantitative atom-probe analysis indicated that the oxide formed during the reaction is stoichiometric Rh<sub>2</sub>O<sub>3</sub>. © 1985 Academic Press, Inc.

### I. INTRODUCTION

The CO oxidation reaction on noble metals exhibits interesting kinetics in its order dependence on partial pressure of the reactant gases (1). On rhodium the order of the reaction in O<sub>2</sub> partial pressure at 500 K changes from positive to negative when the O<sub>2</sub>/CO ratio exceeds values in the range from 20/1 to 40/1. This behavior has been observed on both dispersed particle catalysts (2) and on well-defined Rh(111) surfaces (3). There is strong evidence from both of these studies that this change in order (i.e., deactivation) is due to the formation of some inactive form of oxygen or oxide which poisons the reaction. The oxide-induced deactivation mechanism is also supported by low-pressure studies of the reaction using *in situ* mass spectroscopy (4).

In the study reported here, we have investigated the oxidation of Rh field-emitter surfaces during the CO oxidation reaction. Field-emitter surfaces are advantageous for this type of study because the size and morphology of the surface are comparable to those of a typical, commercial catalyst particle; but, unlike a commercial catalyst par-

ticle, the surface is defined on an atomic scale (5). The study consisted of examining the surface for oxidation following the CO oxidation reaction over a wide range of O<sub>2</sub>/CO ratios. The O<sub>2</sub> partial pressure was kept constant at 1 Torr, and the CO partial pressure was varied from 0.01 to 1 Torr. The conditions required for surface oxidation were determined and correlated with the above conditions where deactivation has been observed. This correlation was used to confirm that the deactivation is oxide induced. Analysis of the oxide was carried out to determine its chemical form.

### II. EXPERIMENTAL

**A. Apparatus.** The apparatus used in this investigation is shown schematically in Fig. 1. The experimental system consists of a reaction chamber, in which reactions are performed at pressures in the range 1–10 Torr and an analysis chamber, in which imaging atom-probe mass spectroscopy (6) and field ion microscopy (5) are carried out at pressures in the low 10<sup>-10</sup>-Torr range. The sample examined with these techniques is a sharply pointed needle called a field emitter or "tip." In our system the tip is spot-welded to the end of a platinum wire

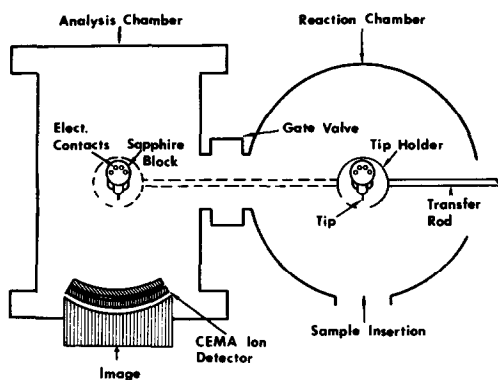


FIG. 1. A schematic drawing of the apparatus used in this study.

loop, and the loop ends are inserted into lengths of nickel tubing running through a cylindrical, sapphire block. The sapphire block is mounted inside a copper cup, and the entire assembly is transferred from one chamber to another on a stainless-steel rod magnetically coupled to the exterior of the vacuum system. During analysis, the rod is detached from the sample assembly, and the analysis chamber is isolated from the reaction chamber by an all-metal gate valve.

The sample can be heated in either chamber by passing a dc current through the platinum wire loop. Two potential leads (0.001-in.-diam. Pt) are used to measure the voltage drop across the center portion of the loop, and the sample temperature is determined by resistance measurements. The details of this temperature control system are discussed in a previous publication (7).

The reactant gases used in this study were spectroscopic grade  $O_2$  and CO supplied from 1-liter glass flasks without further purification. The background pressure in the reaction chamber was typically in the mid  $10^{-9}$ - to low  $10^{-8}$ -Torr range; however, upon sealing off the reaction chamber from the vacuum pumps, the background pressure would slowly increase. During a typical reaction interval (15 min) with 1 to 2 Torr of reactant gases present, the background would probably increase to as much

as  $10^{-5}$  Torr. The primary background gases were CO,  $H_2O$ , and  $H_2$ .

**B. Techniques.** The surface analytical techniques used in this investigation were field ion microscopy and imaging atom-probe mass spectroscopy. Field ion microscopy was used primarily for structural characterization of the surface prior to the reaction. In the field ion technique, the protruding atoms on the apex of the tip are imaged by admitting an inert gas (He and Ne were used in this study) to the analysis chamber and applying a high, positive voltage (5–15 kV is typical) to the tip. The applied voltage produces field strengths at the surface of the order of several volts per Ångström, and this field ionizes the imaging gas atoms above the tip surface. The ions produced in this “field ionization” process are accelerated by the field to an imaging detector (i.e., the channel-plate assembly shown in Fig. 1) where they produce a direct image of the protruding surface atoms. An example of a field ion image from one of the Rh samples used in this investigation is shown in Fig. 2. The dark regions of the image correspond to flat, single-crystal planes, and the concentric circles correspond to atomically stepped regions. The overall size (several hundred Ångströms in tip radius) and morphology of the surface make the field emitter an excellent model of a catalyst particle. Further details concerning the field ion microscope technique can be found in the literature (5).

The chemical composition of the surface following reaction was examined by imaging atom-probe mass spectroscopy. The process which underlies the operation of the atom probe is known as “field desorption” and involves the field-induced removal of surface species. In the imaging atom probe, surface species are desorbed and ionized by applying a high-voltage electrical pulse (2-kV pulses were used in this study) and a dc holding voltage to the tip. The applied voltages produced an instantaneous electric field even higher than that employed for field ion imaging resulting in

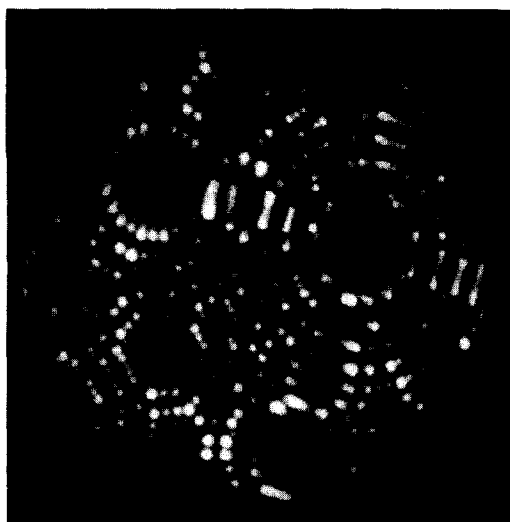


FIG. 2. A field ion image of one of the Rh samples used in this study. Imaging voltage = 5.6 kV, imaging gas =  $2 \times 10^{-5}$  Torr He.

the desorption of surface species. The mass-to-charge ratios of the field-desorbed ions are determined by measuring their flight times from the tip to the channel-plate ion detectors. The flight time measurement is made on the sweep of a transient waveform digitizer. The digitizer trace, which forms the imaging atom-probe mass spectrum, consists of a series of peaks, and the peak intensities give the relative abundances of the field-desorbed species. For more information on the imaging atom probe, the reader is referred to a review article by Panitz (8).

*C. Procedure.* The rhodium field-emitter samples were prepared from 0.005-in.-diameter polycrystalline wire. The tips were sharpened by electropolishing in 4:1 wt/wt ratio of molten  $\text{NaNO}_3 + \text{NaCl}$  at several volts (dc). The samples were introduced into the vacuum system through the reaction chamber and transferred to the analysis chamber for final surface preparation. Surface cleaning was accomplished using a combination of neon cathode sputtering (9) and field evaporation (5). The cathode sputtering technique, which removes contamination from the emitter shank as well as the

apex, was employed to eliminate the possibility of contaminant species migrating from the shank during the reaction. Field evaporation, which is the high-field removal of surface atoms, was used to remove the sputter damage and any remaining contamination from the tip apex. The surface structure was then characterized by field ion microscopy. For the present investigation the analyzed tip apex area was single crystal and the tips were all (100) oriented.

Following the above surface preparation procedure, the tip was transferred to the reaction chamber, and the CO oxidation reaction was carried out. A mixture of  $\text{O}_2$  and CO was admitted to the chamber and the sample was heated. The  $\text{O}_2$  partial pressure was kept constant at 1 Torr, and the CO partial pressure was varied from 0.01 to 1 Torr. The reaction time interval and temperature were 15 min and 500 K, respectively. To terminate the reaction, the sample heating was discontinued followed by removal of the reactant gases.

When the background pressure in the reaction chamber fell to the low  $10^{-7}$ -Torr range, the sample was returned to the analysis chamber. Imaging atom-probe mass spectra were recorded using 2-kV voltage pulses and increasingly higher holding voltages. In a typical experiment, 20–30 mass spectra were recorded. The experiment was completed when all surface species had been removed. The mass spectra obtained were analyzed for the presence of surface oxides.

### III. RESULTS

Mass spectra recorded following heating in equal mixtures of  $\text{O}_2$  and CO gave no indication of surface oxides. The major surface specie detected was CO, and similar mass spectra were observed at increasingly higher  $\text{O}_2/\text{CO}$  ratios up to a ratio of 30/1. An example of an imaging atom-probe mass spectrum taken from a sample heated in a 30/1 mixture is shown in Fig. 3a. The five species identified are associated with ad-

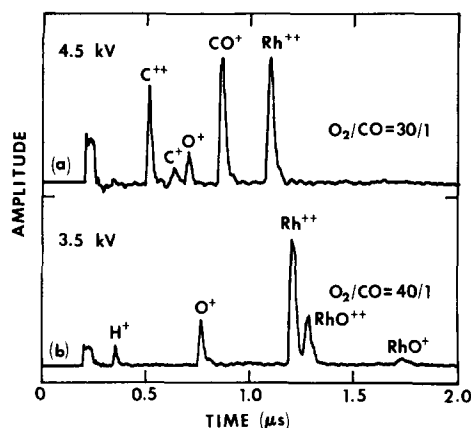


FIG. 3. Imaging atom-probe mass spectra recorded following heating at 500 K in 1 Torr of  $O_2/CO$  mixtures. (a)  $O_2/CO = 30/1$ , (b)  $O_2/CO = 40/1$ . Surface oxides are detected at an  $O_2/CO$  ratio of 40/1.

sorbed CO, CO fragments, and the Rh substrate. Increasing the ratio to 40/1, however, resulted in a qualitative difference in the mass spectra as shown in Fig. 3b. Instead of adsorbed CO, the mass spectra contained signals indicative of a surface oxide. In fact, the four signals observed were identical to the signals observed when the sample was oxidized in pure  $O_2$ . (A systematic study of the oxidation of Rh field emitters has been carried out and will be published elsewhere (10).) The experiment was repeated at ratios of 30/1 and 40/1 several times on two separate samples and the difference in surface composition was absolutely reproducible.

The extent of surface oxidation was found to be a sensitive function of the CO partial pressure. This can be seen in Fig. 4, where the  $CO^+$  and  $RhO^+$  signal intensities are plotted as a function of CO partial pressure. The intensities plotted represent the total signal amplitude for the given species summed over all mass spectra of the experiment. The intensities can be converted to ions detected using a conversion factor of  $\sim 6$  ions/mV (see below). Note that the oxide signal increases from nearly zero to its maximum value as the partial pressure of CO is decreased from 33 to 10 mTorr. The

$CO^+$  signal, which reflects an unoxidized surface, changes from its minimum value to its maximum value over an even narrower range of CO partial pressures.

The chemical form of the oxide was determined by plotting the cumulative number of oxygen ions vs the cumulative number of rhodium ions obtained from successive mass scans through the oxide layer. In imaging atom-probe mass spectra, the peak height of a given signal is proportional to the number of ions of that species desorbed (8). A procedure for converting peak heights to ions desorbed has recently been developed (7), and we have applied this procedure to rhodium and oxygen ions. The proportionality constant was determined to be  $6 \pm 1$  ions/mV for our experimental conditions. Within this experimental error, the proportionality constant was the same for all species and for the entire range of applied voltages required to remove the oxide. Figure 5 shows a cumulative plot taken from a sample heated to 500 K in a 100/1  $O_2/CO$  mixture. The plot is linear initially, where the oxide desorbs exclusively, and has a slope of 3/2 indicative of stoichio-

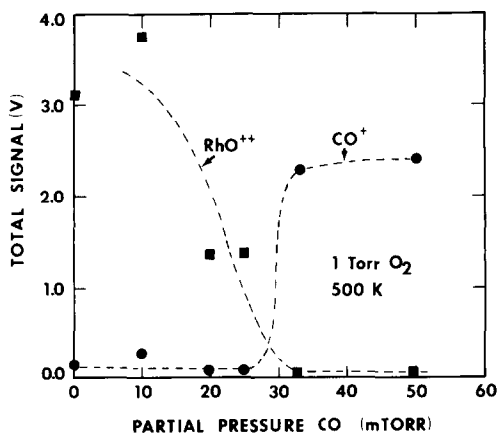


FIG. 4. The total signal intensity for  $RhO^+$  and  $CO^+$  as a function of the CO partial pressure at fixed  $O_2$  partial pressure (1 Torr) and temperature (500 K). The surface oxidizes when the CO partial pressure is 25 mTorr or below. At higher CO partial pressures CO is the predominant surface species remaining after reaction.

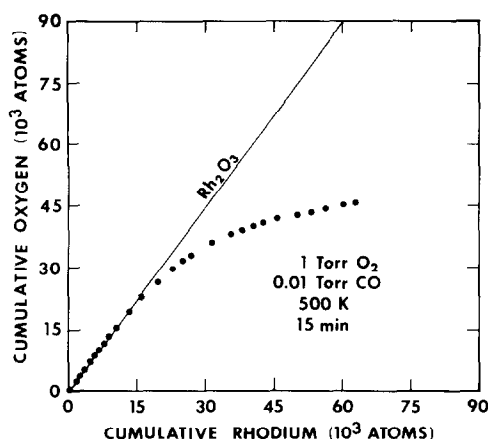


FIG. 5. A plot of the cumulative number of oxygen ions vs the cumulative number of rhodium ions obtained from imaging atom-probe mass spectra recorded after heating in a 100/1  $\text{O}_2/\text{CO}$  mixture at 500 K. The initial slope of 3/2 indicates that the oxide is stoichiometric  $\text{Rh}_2\text{O}_3$ .

metric  $\text{Rh}_2\text{O}_3$ . Note that this compositional analysis is only valid for the outer oxide. As the oxide is removed and the interface is approached, both oxide and metal may desorb simultaneously giving an erroneous composition for the oxide at the interface. At lower  $\text{O}_2/\text{CO}$  ratios, the data were more limited due to the presence of less oxide, but all data from experiments where the  $\text{O}_2/\text{CO}$  ratio was 40/1 or greater were consistent with  $\text{Rh}_2\text{O}_3$  being present on the surface.

#### IV. DISCUSSION

The above results have identified the conditions of reactant partial pressures which result in the oxidation of Rh at 500 K. The 30/1-to-40/1 range of  $\text{O}_2/\text{CO}$  ratios where oxides were detected correlates well with the ratio found for deactivation of the CO oxidation reaction. In a study of the CO oxidation reaction on a 0.01 wt% Rh/ $\text{Al}_2\text{O}_3$  catalyst, Oh and Carpenter (2) found that the  $\text{CO}_2$  production rate first increases and then decreases under net oxidizing conditions. The CO concentration was held fixed at 0.3%, and deactivation occurred at 500 K when the oxygen concentration reached

10%. This condition represents an  $\text{O}_2/\text{CO}$  ratio of 33/1 in excellent agreement with our findings for surface oxidation. The same study (2) also reported evidence for the formation of surface oxides during the CO oxidation reaction. Using X-Ray Photoelectron Spectroscopy (XPS), the catalyst particles were examined following the CO oxidation reaction at 573 K and various  $\text{O}_2/\text{CO}$  mixtures. Because the temperature was significantly higher than that used in our study, a direct comparison between the two studies is not possible. However, even allowing for the higher temperature, the two experiments differ significantly. Whereas we found no evidence for surface oxidation at  $\text{O}_2/\text{CO}$  ratios of 30/1 or below, the XPS study indicated that the surface was oxidizing at a ratio of 2.5/1. If surface oxidation is indeed responsible for deactivation, the XPS result implies that the reaction should deactivate at an  $\text{O}_2/\text{CO}$  ratio of 2.5/1 and a temperature of 573 K. Unfortunately, their reaction rate data showing deactivation was not taken for temperatures higher than 518 K. The conditions required for oxidizing our field-emitter samples at higher temperatures will be explored in the near future.

The 30/1-to-40/1 ratio for surface oxidation also correlates with the deactivation of the reaction on the Rh(111) plane. In a study reported by Fisher and Goodman (3), the  $\text{CO}_2$  production rate at 500 K was found to increase up to an  $\text{O}_2/\text{CO}$  ratio of 20/1 and decrease at a ratio of 40/1. Auger Electron Spectroscopy was used to examine the surface following the reaction, and, in agreement with our results, evidence for surface oxygen was found only when the  $\text{O}_2/\text{CO}$  ratio exceeded deactivation conditions. The excellent agreement between the two experiments, which were performed on such different types of surfaces, is a good indication that surface structure does not play a significant role in the deactivation process.

#### V. SUMMARY

Surface oxides form on Rh field emitters during the CO oxidation reaction at 500 K

when the  $O_2/CO$  ratio is 40/1 or higher. That these conditions correlate with the deactivation of the reaction is confirming evidence that oxide formation is the surface process responsible for deactivation. The chemical form of the oxide is identified as stoichiometric  $Rh_2O_3$ . The strongly oxidizing conditions required to produce surface oxides obviously represent conditions where surface oxygen is building up faster than it can be removed by reaction with adsorbed CO. At higher temperatures, thermal desorption of CO will reduce the CO oxidation rate, produce a higher concentration of surface oxygen, and cause the surface to oxidize at lower  $O_2/CO$  ratios. A study of the temperature dependence of the  $O_2/CO$  ratio required for oxide formation is planned for the near future, and, upon completion of the experiments, we will determine if the process can be modeled by a set of simple, coupled rate equations.

#### ACKNOWLEDGMENTS

The author acknowledges D. W. Goodman for several helpful discussions relating to the CO oxidation

reaction, J. T. Yates, Jr. for a critical reading of the manuscript, J. A. Panitz for advice relating to the imaging atom-probe technique, and L. M. Karkiewicz for his technical assistance. This work was performed at Sandia National Laboratories supported by the U.S. Department of Energy under Contract DE-AC04-76DP00789.

#### REFERENCES

1. Cant, N. W., Hicks, P. C., and Lennon, B. S., *J. Catal.* **54**, 372 (1978).
2. Oh, S. H., and Carpenter, J. E., *J. Catal.* **80**, 472 (1983).
3. Fisher, G. B., and Goodman, D. W., to be published.
4. Kim, Y., Shi, S.-K., and White, J. M., *J. Catal.* **61**, 374 (1980).
5. Müller, E. W., and Tsong, T. T., "Field Ion Microscopy: Principles and Applications." Elsevier, New York, 1969.
6. Panitz, J. A., *Rev. Sci. Instrum.* **44**, 1043 (1973).
7. Kellogg, G. L., *Phys. Rev. B* **29**, 4304 (1984).
8. Panitz, J. A., in "Progress in Surface Sciences" (S. G. Davison, Ed.), Vol. 8, Part 6. Pergamon, New York, 1973.
9. Cranstoun, G. K. L., Browning, D. J., and Pyke, D. R., *Surf. Sci.* **34**, 597 (1973).
10. Kellogg, G. L., *Phys. Rev. Lett.* **54**, 82 (1985).